LIMNOLOGY
and
OCEANOGRAPHY

Massive circumpolar biomass of Southern Ocean zooplankton: Implications for food web structure, carbon export, and marine spatial planning

Guang Yang [1,2,3]* Angus Atkinson [4] Evgeny A. Pakhomov [5,6,7] Simeon L. Hill [8] Marie-Fanny Racault [9]

[1]Key Laboratory of Marine Ecology and Environmental Sciences, Institute of Oceanology, Chinese Academy of Sciences, Qingdao, People's Republic of China
[2]Laboratory for Marine Ecology and Environmental Science, Qingdao National Laboratory for Marine Science and Technology, Qingdao, People's Republic of China
[3]Center for Ocean Mega-Science, Chinese Academy of Sciences, Qingdao, People's Republic of China
[4]Plymouth Marine Laboratory, Plymouth, UK
[5]Department of Earth, Ocean, and Atmospheric Sciences, University of British Columbia, Vancouver, British Columbia, Canada
[6]Institute for the Oceans and Fisheries, University of British Columbia, Vancouver, British Columbia, Canada
[7]Hakai Institute, Campbell River, British Columbia, Canada
[8]British Antarctic Survey, High Cross, Cambridge, UK
[9]School of Environmental Sciences, University of East Anglia, Norwich, UK

Abstract

With rapid, sector-specific climatic changes impacting the Southern Ocean, we need circumpolar-scale biomass data of its plankton taxa to improve food web models, blue carbon budgets and resource management. Here, we provide a new dataset on mesozooplankton biomass with 2909 records spanning the last 90 yr, and describe, in comparable carbon units, their circumpolar distribution alongside those of phytoplankton, Antarctic krill, and salps. With our datasets, we estimate total summer carbon biomasses for phytoplankton (36 MT), mesozooplankton (67 MT), krill (30 MT), and salps (1.7 MT). The mesozooplankton value is much higher than previously reported and, added to that of krill and salps, points to an enormous overall biomass of zooplankton in the Southern Ocean. This means that the pyramids of biomass are often inverted, with higher biomass of zooplankton than of phytoplankton. Such high biomasses suggest key roles of grazers in nutrient cycling and we estimate an export of ~ 50 Mt C yr^{-1}, solely from mortality of overwintering zooplankton that typically reside at depth. Deep lipid respiration (the lipid pump), for example, would increase this export even further. While inverted biomass pyramids prevailed at mid latitudes (50°–70°S), the balance of taxa differed regionally: for example, with biomass dominance by phytoplankton (highest latitudes and Pacific sector), mesozooplankton (Kerguelen Plateau), krill (north and east Scotia Sea), and salps (Crozet area). In light of contrasting climate change impacts between these sectors, we provide data that will underpin biogeochemical and food web models, blue carbon budgets, and the planning of marine protected areas.

*Correspondence: yangguang@qdio.ac.cn

Aspirations for improved understanding of food webs, biogeochemical cycles, and marine protection networks around Antarctica require circumpolar-scale, comparative biomass data on the basal trophic groups. So far, however, these basic underpinning data have been incomplete or lacking (Johnson et al. 2022). Nevertheless, our circumpolar perspective on Southern Ocean ecosystems suggests very different food web structures between sectors (Hill et al. 2021; McCormack et al. 2021) concomitant with contrasting rates and directions of environmental change (Morley et al. 2020; Parkinson and Cavalieri 2012; Stammerjohn et al. 2012). These differences in food web structure persist despite strong connectivity between

sectors (Murphy et al. 2021), and it has been argued that this connectivity requires a circumpolar network of protected areas (Brooks et al. 2020; Cavanagh et al. 2021). To facilitate planning of this network, the Commission for the Conservation of Antarctic Marine Living Resources (CCAMLR) has defined nine broad marine protected area (MPA) planning domains around Antarctica, based on the location and scale of geographically distinct research activities (Fig. 1a).

Some high-latitude embayments of the Southern Ocean, such as the Ross Sea MPA and proposed Weddell Sea MPA, have already had thorough appraisal of data to underpin protection goals (Teschke et al. 2020). Brooks et al. (2020), argued that MPAs need to conserve the full range of biodiversity, but at the larger, circumpolar scale of the nine MPA planning domains, the information on biodiversity and bioregionalization is still very incomplete. Most efforts so far to define circumpolar ecological structure have been based either on the physical properties of the ecosystem or on the distribution of a single trophic level (Pinkerton et al. 2020). The most recent analysis of physical variables identified 20 distinct bioregions based on surface temperature, depth, and sea ice cover (Raymond 2011). "Areas of ecological significance" (AES), have also been recognized, based on tracking of air-breathing vertebrates (Hindell et al. 2020). However, these predators form only one component of the food web, and since they are usually tagged in accessible onshore breeding colonies, they may provide an incomplete representation of these species' use of habitat (Ratcliffe et al. 2021). Several studies have also presented circumpolar scale views of lower trophic level groups including phytoplankton (Arrigo et al. 2008; Deppeler and Davidson 2017; Pinkerton et al. 2021), mesozooplankton (Foxton 1956; Moriarty and O'Brien 2013; Pinkerton et al. 2020), salps (Foxton 1966; Pakhomov et al. 2002), and krill (Marr 1962; Atkinson et al. 2008; Atkinson et al. 2009). However, in common with the higher predator tracks, most of these studies only applied to a narrow subset of the food web.

The purpose of this paper is to provide a wider appraisal of the base of the food web, by conducting a circumpolar-scale, comparative biomass analysis across major plankton groups, from phytoplankton up to krill and salps. We provide the Southern Ocean scale distributions of four basal plankton functional groups, namely phytoplankton, mesozooplankton, Antarctic krill (*Euphausia superba*), and salps (mainly *Salpa thompsoni*). Although a few previous studies compare multiple groups quantitatively at circumpolar scales (Voronina 1998; Pakhomov et al. 2002; Atkinson et al. 2004), this paper also presents a large new database on mesozooplankton biomass, allowing a comparison of the four main plankton functional groups in equivalent carbon biomass units. This provides quantitative baseline information on pelagic food web structure to underpin spatial protection planning across the nine MPA planning domains. Being in carbon units and pertaining to key functional groups, we have tailored our data to help construct large scale budgets and models of food web transfer

and carbon cycling (Le Quéré et al. 2016; Karakus et al. 2021), thus supporting efforts to quantify potential "blue" carbon routes to sequestration.

Data and methods

Overview of data sources

To make a circumpolar scale comparison of the plankton tractable, we have compiled all available data from the open water summer season (December to March) to produce long-term biomass "climatologies" of four major functional groups of plankton, namely phytoplankton (estimated from satellite-derived chlorophyll a [Chl a]), and three zooplankton groups (estimates from net samples): mesozooplankton (mainly small metazoan zooplankton, dominated by copepods and excluding Antarctic krill and salps), Antarctic krill (*Euphausia superba*) and salps (aggregates and solitaries of all species). Table 1 summarizes the sampling coverage of each functional group.

Our source of Chl a data is the European Space Agency Ocean Color Climate Change Initiative (ESA OC-CCI) (Mélin et al. 2017; Sathyendranath et al. 2019). The krill and salp data are sourced from KRILLBASE (Atkinson et al. 2017). For the mesozooplankton, we compiled a large new database which we present in Supporting Information Data S1 to make it available for wider use. This is built partly from the foundations of an earlier existing database (Moriarty and O'Brien 2013), comprising 1125 stations, and with an additional 1784 stations added. These metadata are available via the present paper which needs to be cited as the original source and detailed descriptions of the column headings are shown in Supporting Information Table S1 (Data S2). Below we describe each source of data in more detail.

Chl a and phytoplankton

Long-term average satellite Chl a concentrations (mg Chl a m^{-3}) in the circum-Antarctic study region (i.e., south of 40°S) were obtained for all complete years of coverage (January to December), over austral summer (December, January, February, and March) and each month of summer from 1998 to 2020. These values were extracted based on 4 km resolution blended Chl a data product OC-CCI version 4.2 and gridded to a 0.5° latitude × 1° longitude grid. The OC-CCI V4.2 merges data from the Sea-Viewing Wide-Field-of-View Sensor, the Aqua Moderate-Resolution Imaging Spectro-Radiometer, the Medium Spectral Resolution Imaging Spectrometer, and the Suomo-NPP Visible Infrared Imaging Radiometer Suite into a unified, bias-corrected, and climate-quality-controlled product.

For a simple and direct circumpolar-scale comparison of phytoplankton and zooplankton carbon standing stocks, we converted mg Chl a m^{-3} to units of g C m^{-2}. To convert first from concentrations per m^3 within the surface layer to a depth-integrated value, we used a series of spring, summer, and autumn transects across the Scotia Sea in Korb et al. (2012) which compared both surface and depth integrated
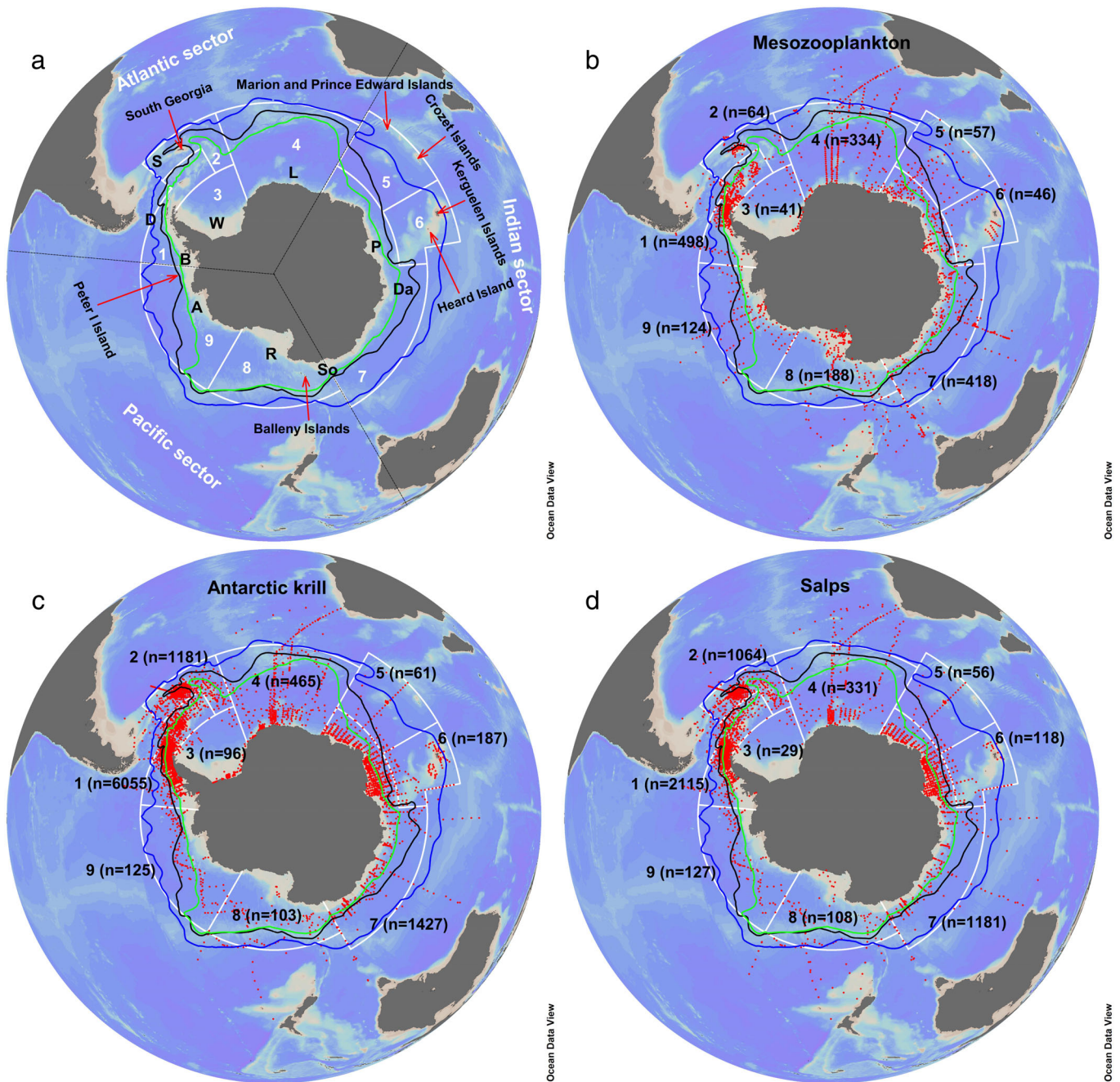
Fig. 1. Geographic location of main seas, islands, fronts and CCAMLR planning domains (marked with numbers 1–9, http://gis.ccamlr.org) in the Southern Ocean (**a**) and distribution of summer (December to march) sampling stations of mesozooplankton in this dataset (**b**) and krill (**c**) and salps (**d**) in KRILLBASE (Atkinson et al. 2017). 1, Western Antarctic Peninsula-South Scotia Arc; 2, North Scotia Arc; 3, Weddell Sea; 4, Bouvet-Maud; 5, del Cano-Crozet; 6, Kerguelen Plateau; 7, East Antarctica; 8, Ross Sea; 9, Amundsen-Bellingshausen. Main fronts such as Antarctic Polar Front, Southern Antarctic Circumpolar Current (ACC) Front and Southern Boundary of ACC are marked in blue, black and green, respectively. (**a**) A, Amundsen Sea; B, Bellingshausen Sea; D, Drake Passage; Da, Davis Sea (82°–96°E); L, Lazarev Sea (0°–14° E); P, Prydz Bay; R, Ross Sea; S, Scotia Sea; So, Somov Sea (150°–170° E); W, Weddell Sea. The Atlantic sector, Indian sector, and Pacific sector are divided based on longitudinal boundaries of MPA planning domains 1–4 (85°W–30°E), 5–7 (30°–150° E), and 8–9 (150°E–85°W), respectively. (**b–d**) Number of stations in each CCAMLR planning domain are shown in parentheses. These circumpolar maps are produced in Ocean Data View (Schlitzer 2021).

values (their table 2), across a range of water masses. Based on a median value from these 12 pairwise comparisons we used a multiplication factor of 41 (range: 22–96) to convert near-surface Chl *a* values (mg Chl *a* m^{-3}) to depth integrated values (mg Chl *a* m^{-2}) values. Second, to convert from Chl *a* to C units we used a C : Chl *a* ratio of 60.5 (based on median value

Table 1. Summary of sampling coverage during summer (December to March).

	Phytoplankton	Mesozooplankton	Antarctic krill	Salps
Sampling years (no. of years)	1998–2020 (23)	1932–2020 (61)	1926–2016 (54)	1926–2009 (44)
Total no. of stations (no. in domains 1–9)	N/A	2028 (1770)	9907 (9700)	5432 (5129)

for a range of regions and determinations listed in table 4 of Sathyendranath et al. 2009).

Mesozooplankton
Origin of data

The mesozooplankton biomass database was compiled from a combination of an existing database, published papers, cruise reports, and unpublished data of the authors. A total of 5916 net hauls were compiled initially in our full database, with 2310 of these derived from the existing mesozooplankton biomass database for the global ocean (Moriarty and O'Brien 2013). Although these data are reported in a variety of units, all are standardized by volume. Some of the hauls formed part of a depth-stratified series of nets or repeating sampling made at a single station. To better compare mesozooplankton biomass across regions, we simplified the full dataset to replace each depth-stratified series with a single, depth-integrated estimate. This was the sum of the depth-stratified values except when there were multiple hauls from the same depth stratum, which we averaged using the arithmetic mean before summing across strata. This reduced the full dataset to 2909 stations (Supporting Information Data S1). In this study, we used data spanning from December to March (2028 stations). These reduced data are circumpolar in scope (Fig. 1) and span 61 yr (Table 1).

For each of the component net hauls in the database, we compiled a suite of parallel sampling information. This included station longitude and latitude; sampling date; top and bottom depth of net haul; record type; net type including mesh size; original biomass value and units, method used to derive the biomass (if available); and origin of the data. Supporting Information Table S1 (Data S2) describes these data fields in more detail.

During the source dataset compilation, we found a discrepancy between the existing mesozooplankton biomass database (mean: 0.046 mL m^{-3}, 0–250 m, $n = 245$; Moriarty and O'Brien 2013) and some of its raw source data, namely the *Discovery Investigations* (1932–1951) records (mean: 0.037 mL m^{-3}, 0–250 m, $n = 245$) from Foxton (1956). To make our dataset more traceable, we recompiled Foxton's (1956) data based on the original records of displacement volume (DV) measured on each net sample. Volumes of seawater filtered for each record in Foxton (1956) were estimated based on the mouth of Nansen closing net (N70V, 70 cm) and distance traveled of the tow. All post-war catches (21 records in 1951) were multiplied by 1.5 following Atkinson (1991) because a different design of net was used during the post-war sampling.

The database has data from nets of variable mouth area, towing depth, and mesh size. To make the data more comparable, the original biomass data were first converted to carbon biomass (mg C m^{-3}), then standardized to equivalent values in the top 200 m of the water column, and finally converted to equivalent 200-μm mesh values. These sequential adjustments are described below.

Biomass unit standardization

Five kinds of biomass type exist within our compiled records: DV (mL m^{-3}, $n = 933$ stations), dry mass (DM, mg m^{-3}, $n = 812$ stations), wet mass (WM, g m^{-3}, $n = 787$ stations), settled volume (SV, mL m^{-3}, $n = 258$ stations), and carbon mass (CM, mg C m^{-3}, $n = 119$ stations). DV, settled volume, and WM were usually used in early Southern Ocean zooplankton biomass studies (Foxton 1956).

We converted these metrics to a single comparable metric, carbon biomass (mg C m^{-3}), which is widely used in food web analysis, biogeochemistry studies and modeling. The initial biomass values with different units were all converted to the standard carbon biomass (mg C m^{-3}) according to nonlinear conversion equations from Wiebe (1988) and Balvay (1987) which were compiled in Moriarty and O'Brien (2013):

$$\log_{10}(CM) = \left[\log_{10}(DV) + 1.434\right]/0.820,$$
$$\log_{10}(DM) = \left[0.843 \times \log_{10}(SV)\right] + 1.417,$$
$$\log_{10}(CM) = \left[\log_{10}(WM) + 1.537\right]/0.852,$$
$$\log_{10}(CM) = \left[\log_{10}(DM) - 0.499\right]/0.991,$$

where CM is carbon biomass (mg C m^{-3}), DV is displacement volume (mL m^{-3}), DM is dry mass (mg m^{-3}), SV is settled volume (mL m^{-3}), and WM is wet mass (g. m^{-3}).

Depth standardization

We standardized biomass estimates to a water depth chosen to represent the biomass in the epipelagic zone, here defined as 0–200 or 250 m. The latter is the main depth threshold for stratified sampling in the *Discovery* era (1926–1939) while 200 m is the main threshold in the modern era. Consequently, there is a lack of overlapping data to use in inter-calibrating the two depth ranges. For this reason, we made the pragmatic decision not to attempt to convert values to a single depth, but retained both 200 and 250 m as the lower depth interval.

Foxton (1956) presented a circumpolar assessment of the biomass of zooplankton sampled from various depth strata (0–50, 50–100, 100–250, 250–500, 500–750, and 750–1000 m). To standardize the original-type biomasses according to depth, we calculated a series of month-specific ratios of biomass in each cumulative stratum to the biomass in the 0–250 m stratum (Supporting Information Table S2; Data S2) based on Foxton (1956). Thus, all original

records were assigned to one of Foxton's depth strata on the basis of sampling depth. The month-specific ratios were based in DV, so we retained the DV information in this assignment of hauls to strata. We then standardized to the 0–250 m stratum according to the month-specific ratio and then converted to carbon biomass (g C m^{-2} within the top 250 m layer).

Mesh size conversion

The dataset we compiled includes zooplankton records collected using various net types with mesh size ranging from 100 to 500 μm. The 200-μm mesh net, which was most commonly used, forms a good comparison across studies so we used this size as a benchmark (Atkinson et al. 2012). A mesh category grouped by 125, 153, 200, 280, 330, and 500 μm was assigned to each record according to its original mesh size (the nearest value) and all the carbon biomass values were converted to its equivalent 200 μm values using linear mesh conversion equations (Gallienne and Robins 2001; Atkinson et al. 2012; Moriarty and O'Brien 2013).

$$CM_{M125} = 1.25623 \times CM_{M200},$$

$$CM_{M150} = 1.14296 \times CM_{M200},$$

$$CM_{M280} = 0.83435 \times CM_{M200},$$

$$CM_{M330} = 0.75899 \times CM_{M200},$$

$$CM_{M500} = 0.51169 \times CM_{M200},$$

Krill and salps

Carbon biomasses of krill and salps were calculated based on abundance (no. ind. m^{-2}) from KRILLBASE (Atkinson
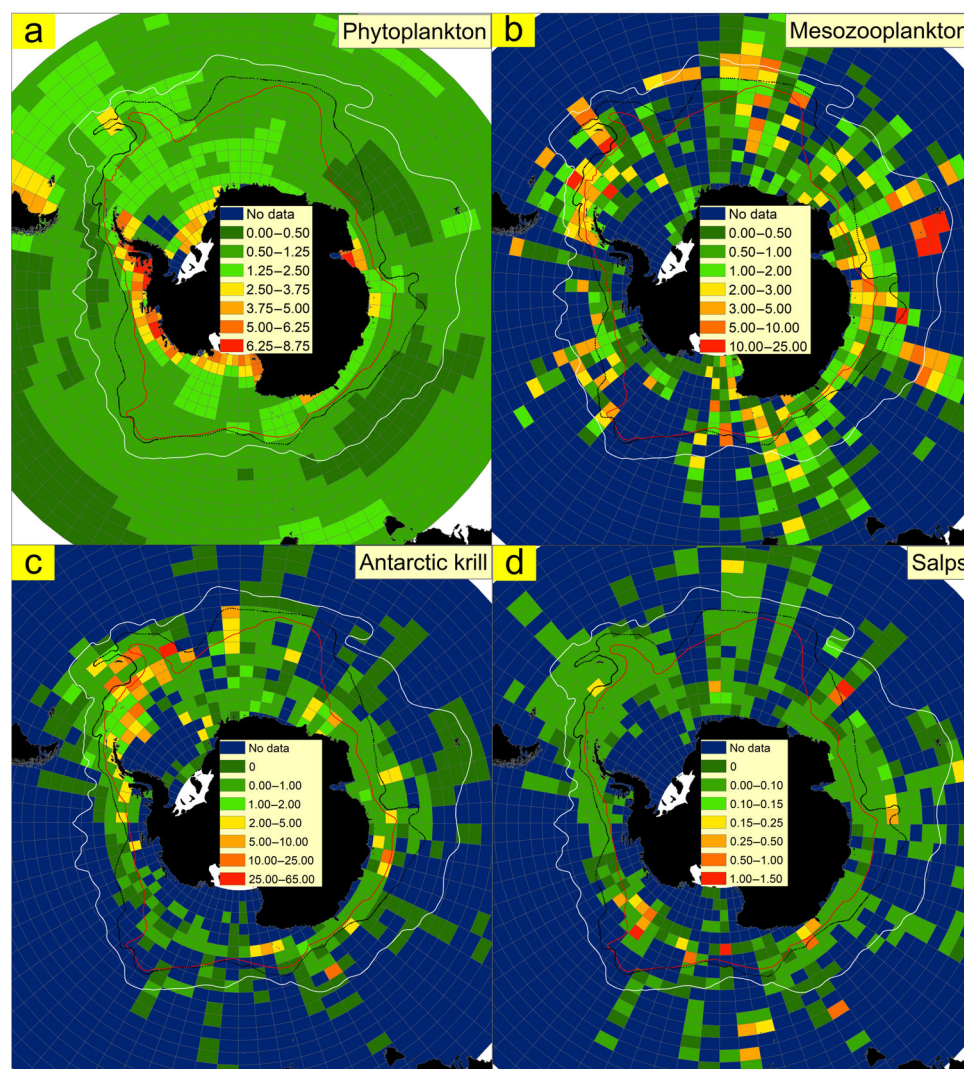
Fig. 2. Distribution and carbon biomass (g C m^{-2}) of phytoplankton (**a**), mesozooplankton (**b**), krill (**c**), and salps (**d**) with grid size of 2° latitude by 5° longitude. General location of the major fronts (Polar Front, Southern Antarctic Circumpolar Current Front and Southern Boundary of Antarctic Circumpolar Current) is marked in white, black, and red, respectively (Orsi et al. 1995). The phytoplankton plot (**a**) is based on multiyear summer mean Chl *a* value (December to March, 1998 to 2020, ESA OC-CCI data). Mesozooplankton (**b**), krill (**c**), and salps (**d**) plots are based on summer data (December to March) of our new data set and KRILLBASE (Atkinson et al. 2017).

et al. 2017) using a fixed conversion factor from numbers to biomass for each taxon. We screened the data to include only summer hauls (spanning December to March) with a top sampling depth shallower than 20 m and bottom sampling depth deeper than 50 m. For salps, summer data (December to March) with no limit set on top depth and bottom sampling depth deeper than 100 m was used. These screenings were selected for consistency with previous work (Atkinson et al. 2017) and yielded a total of 9907 records for krill and 5432 records for salps at a circumpolar scale (Fig. 1c,d; Table 1). Because of the ability of krill to evade nets, we used standardized abundance values (i.e., to a 0–200 m night-time, 8 m^2 rectangular midwater trawl [RMT 8] haul on 01 January). Abundance values for salps were not standardized (Atkinson et al. 2017).

Based on the WM value of krill, length frequency and aggregate/solitary ratio data of salp (Foxton 1966), and equations provided in the published literature (Atkinson et al. 2009, 2012; Dubischar et al. 2012), conservative carbon mass values of 48.25 mg C ind^{-1} for krill and 0.819 mg C ind^{-1} for salps were used to convert numerical densities to biomass densities (Supporting Information Data S3).

Data presentation in the context of marine protected areas

CCAMLR have defined nine marine protected area planning domains around Antarctica (Fig. 1). In addition to providing a circumpolar perspective on the lower trophic levels, we have also presented the biomass data averaged according to these MPA planning domains (Fig. 1; Table 1) to find the spatial contrasts in the relative balance of the key functional groups at the base of food web.

Results

Circumpolar distributions of the planktonic functional groups

Based on a 2° latitude × 5° longitude grid, we have plotted the climatological mean distributions of phytoplankton, mesozooplankton, krill, and salps in Fig. 2.

High phytoplankton biomass regions were mainly distributed in neritic areas with polynyas, for example, the Ross Sea, Prydz Bay, Amundsen Sea, Bellingshausen Sea, and west of Antarctic Peninsula (Figs. 2a; Supporting Information Fig. S4, Data S2). Mesozooplankton biomass hotspots were mainly distributed near to islands such as Kerguelen, Heard Island, South Georgia, South Shetland Islands, Peter I Island, and Balleny Islands (Fig. 2b), which are all sources of iron fertilization. Hotspots of Antarctic krill were mainly concentrated in the Atlantic sector (Fig. 2c, see also Atkinson et al. 2008, 2017). Salps were mainly distributed in low latitudes, although some salp hotspots in the Pacific Sector lie inside the Southern Boundary of the ACC (Fig. 2).

Total circumpolar biomass of the four plankton functional groups

Total summer epipelagic biomasses for mesozooplankton, krill, and salps (summed across planning domains) were 67, 30, and 1.7 MT carbon. This clearly shows the domination of mesozooplankton at the circumpolar scale. The average Southern Ocean biomass values for mesozooplankton, krill, and salps across all stations for each zooplankton group (Fig. 1) suggest circumpolar carbon densities of to 1.94, 1.79, and 0.04 g C m^{-2}, respectively. For comparison the phytoplankton value, calculated as the mean of all cells south of 40°S, is 1.03 g C m^{-2}.

Figure 3 also illustrates the generally high carbon standing stock of zooplankton compared to phytoplankton. This is most pronounced in mid Antarctic latitudes, where large areas have summer zooplankton biomass more than double the estimated value of phytoplankton.

Latitudinal zonation of planktonic groups

For this analysis we divided the Southern Ocean into three broad longitudinal sectors (Atlantic, Indian, Pacific) whose
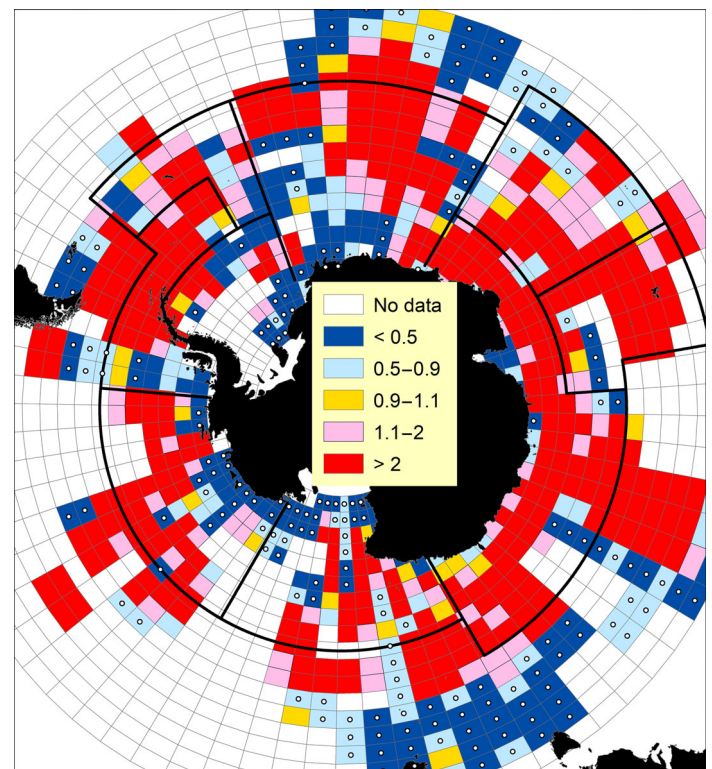
Fig. 3. Regional patterns of bottom-heavy (phytoplankton dominated) or top-heavy (zooplankton dominated) biomass pyramids, indicated by ratio between the sum of average carbon biomass of grazers (mesozooplankton, krill plus salps) and the mean carbon biomass of phytoplankton in each cell with 5° longitude × 2° latitude. Boundaries of the nine domains are shown with black line. Mesozooplankton data were available for each of the colored cells, but the availability of krill and salp data varied. Cells with white dots indicate a ratio < 0.9 based on data for < 3 zooplankton groups (i.e., the bottom-heaviness is uncertain).

boundaries correspond partially to domain edges. Because latitude is a poor proxy for water temperature around Antarctica due to the continent being offset from the south pole, we have used major water masses defined by frontal mean positions (Orsi et al. 1995) as a basis for the zonal distribution for the taxa within each of the three sectors (Fig. 4).

Phytoplankton biomass peaked at the highest latitudes south of the Southern Boundary of the Antarctic Circumpolar Current (SB-ACC, Figs. 2, 4; Supporting Information Fig. S2, Data S2). Mesozooplankton peaked at low and mid latitudes (Fig. 4; Supporting Information Fig. S2, Data S2). Krill and salps also reached a peak at mid latitudes between the PF and the SACCF (Fig. 4; Supporting Information Fig. S2, Data S2). Salps were notably abundant south of the SB-ACC in the Atlantic sector and Pacific sector with a few hotspots also located south of the SB-ACC in Indian sector (Fig. 2) (see Fig. 1. for details of fronts).

### Relative balance of the four plankton functional groups between planning domains

Figure 5 presents these distributions as summary mean biomass density values for the nine MPA planning domains depicted in Fig. 1. There are clearly major differences between domains, and each taxon except salps has a clear maximum value in one of the domains: domain 3 for phytoplankton,

domain 6 for mesozooplankton with very high concentrations in the Kerguelen area, domain 2 for krill. In contrast to krill, the highest salp biomasses were outside the Atlantic sector in domains 5, 8, and 9 (Fig. 5).

Figure 6 puts the four functional groups into the same units (g C m^{-2}) to provide a broad comparison of their relative biomass across the nine MPA planning domains. The planning domains contrast greatly; for instance, krill biomass in domains 2 and 3 exceeds that of mesozooplankton while in other domains the mesozooplankton biomass exceeds that of krill. Likewise, krill and salp dominance contrast between domains 2 and 5, while the high phytoplankton values in the coastal Weddell Sea domain 4 contrast with its open-ocean neighbor domain 5.

Are long-term climatologies representative of the recent past?

The temporal coverage is different between the satellite data for Chl *a*, which covers the period since 1998, and the zooplankton data which span 90 yr with most of the sampling conducted from 1926 to 1939 and from 1976 to present. The degree of background environmental change is therefore different between phytoplankton and zooplankton datasets. To assess the impact of these differences on our comparison of biomass based on long-term averages,
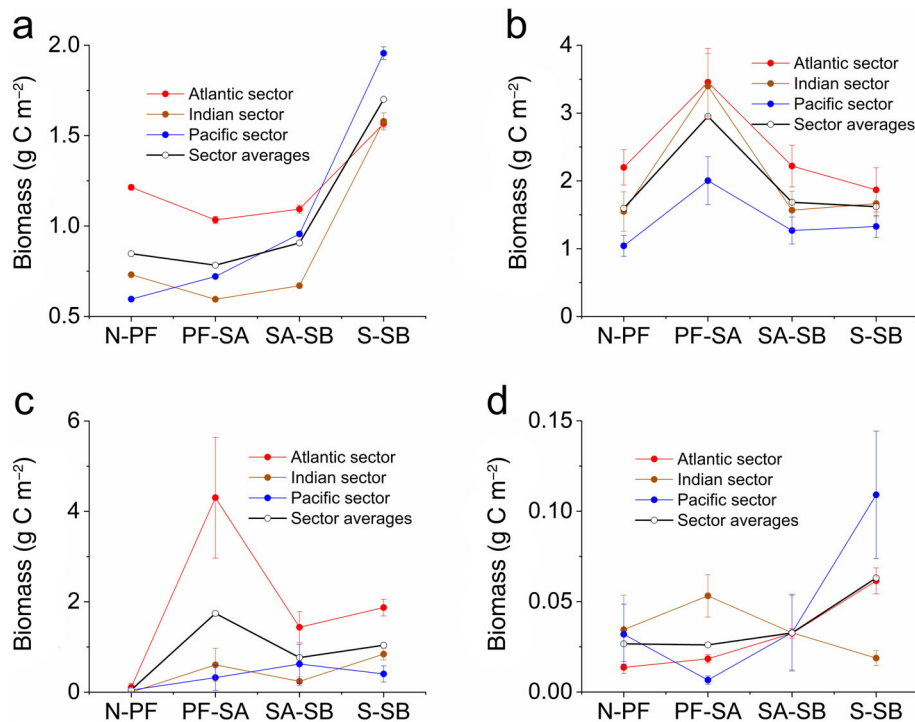
Fig. 4. Mean and SE of carbon biomass (g C m^{-2}) of phytoplankton (**a**), mesozooplankton (**b**), krill (**c**), and salps (**d**) across water mass zones defined by mean frontal positions. N-PF, north of Polar Front (PF); PF-SA, between PF and the Southern Antarctic Circumpolar Current Front (SA); SA-SB, between SA and Southern Boundary of the Antarctic Circumpolar Current (SB); S-SB, south of SB. The Atlantic sector, Indian sector, and Pacific sector are divided based on longitudinal boundaries of MPA planning domains 1–4 (85°W–30°E), 5–7 (30°E–150°E), and 8–9 (150°E–85°W), respectively. Sector averages are the averages of the mean value of the three sectors.
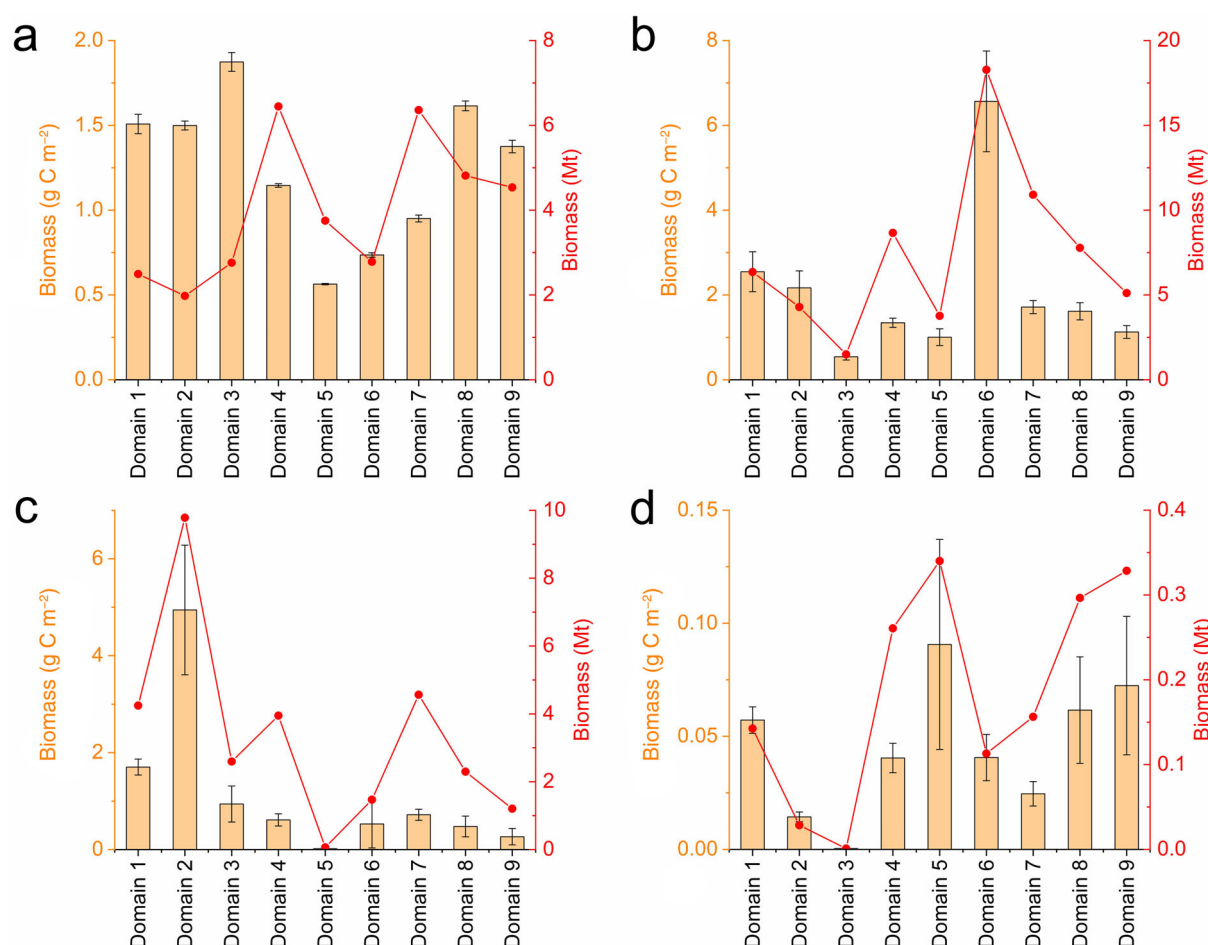
Fig. 5. Mean and SE of carbon biomass (g C m^{-2}, histogram) and overall biomass (Mt, Red line) of phytoplankton (**a**), mesozooplankton (**b**), krill (**c**), and salps (**d**) in each CCAMLR Marine Protected Area planning domains based on summer data (December to March).

Fig. 7 compares the three zooplankton group distributions in the modern era (defined as 1996 onwards; Yang et al. 2020) with those from the previous ~ 70 yr (i.e., spanning 1926–1995). Only four domains had sufficient data for any meaningful comparison (defined here as > 50 records for each of the three zooplankton group in each era; Supporting Information Table S3, Data S2). This analysis shows some features already described such as declines in krill (Fig. 7) particularly in domain 2 (Atkinson et al. 2019; Yang et al. 2020). However, some large differences between eras, for example in mesozooplankton in Domain 1, would require further analysis as more data become available (Fig. 7). This analysis also provides tentative indications of other potential changes such as a decrease in all zooplankton groups in domain 1 and an increase in salps in domain 7. More definitive conclusions are not possible given the sometimes low sample sizes and asymmetrical distribution of data. Notwithstanding these uncertainties, it appears that the rank biomass of krill, salps, and mesozooplankton remained unchanged at the circumpolar scale, that is,

mesozooplankton and salps had the highest and the lowest standing stocks, respectively.

Discussion

Our comparison of the biomass distributions of phytoplankton, mesozooplankton, krill, and salps at a circumpolar-scale builds on a series of foundational studies from last century, most recently Voronina (1998). Our analysis expands the set of trophic groups considered to include phytoplankton and it draws on a much larger dataset than was available to Voronina (1998).

Our data show that the enormous carbon biomass of a single species—Antarctic krill—around Antarctica (30 Mt C) is less than half that of the mesozooplankton (67 Mt C) but 17 times that of salps (1.7 Mt C). These values are similar to the converted carbon biomasses of Antarctic krill (27 Mt) and salps (1.3 Mt, Supporting Information Table S4, Data S2) based on the raw WM data of Voronina (1998) and the species-specific mass conversion factors (Voronina 1998; Atkinson et al. 2012). However, Voronina's
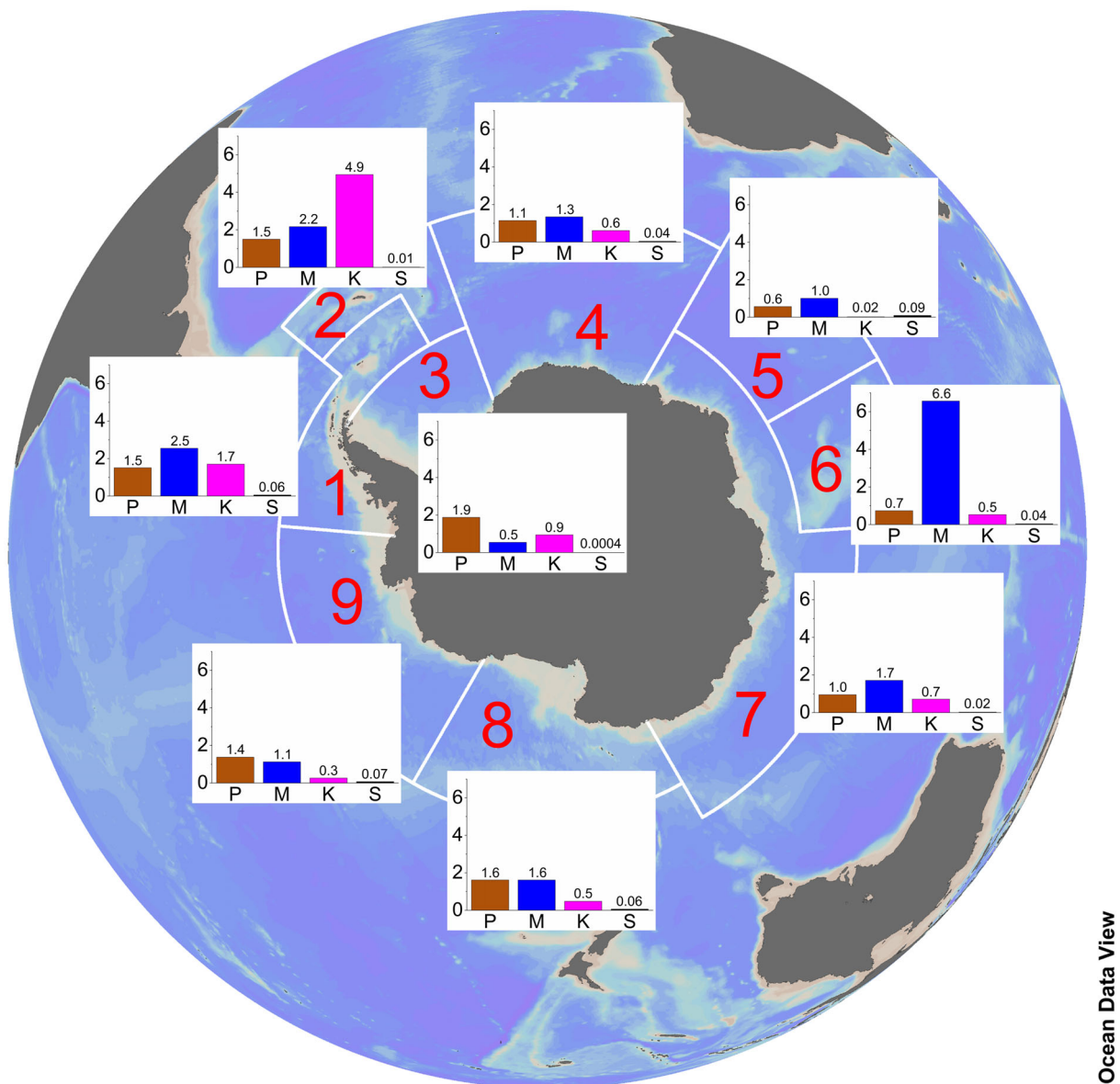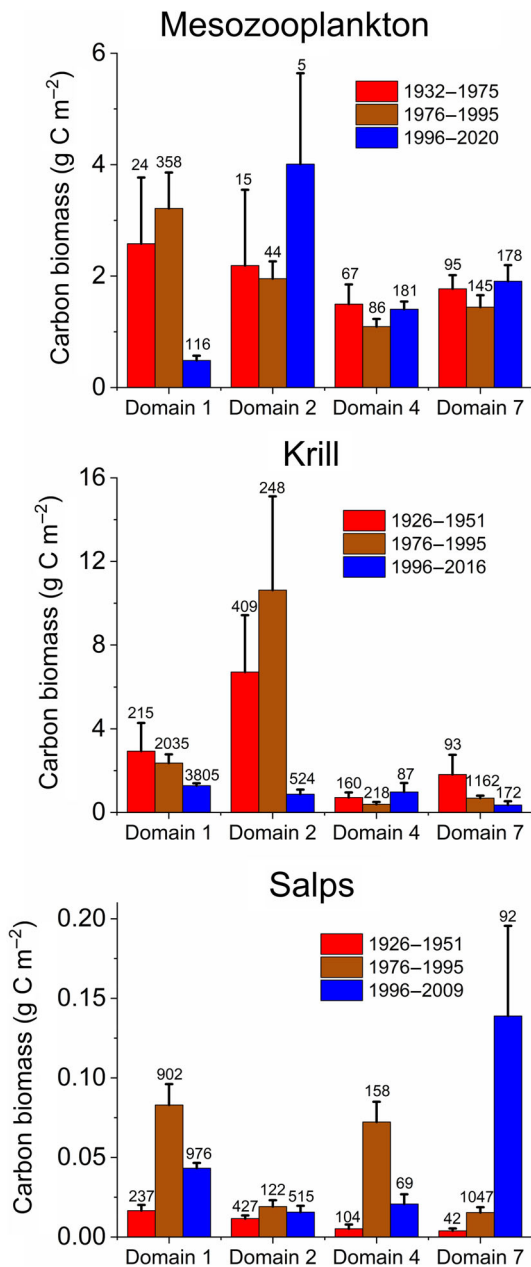
Fig. 6. Comparison of the biomass concentration (g C m^{-2}) of major planktonic functional groups (P, phytoplankton; M, mesozooplankton; K, krill; S, salps) in each CCAMLR Marine Protected Area planning domain. Biomass values for each group are shown on top of each column. These circumpolar maps are produced in Ocean Data View (Schlitzer 2021).

estimate of mesozooplankton biomass, based on 118 stations sampled before 1995 (35 Mt) was less than 60% of our estimate (61 Mt based on our pre-1995 data). Although some previous studies have suggested an increase in the abundance of some dominant copepod species in the contemporary era compared with the Discovery era based on data from east Antarctica (110°E–160°E, Kawamura 1986) and the Scotia Sea (Ward et al. 2018), this is not fully reflected in our mesozooplankton data (Fig. 7) and our much larger sample size (Supporting Information Table S4, Data S2) may be the main factor explaining the difference between Voronina's and our estimates of mesozooplankton biomass.

Assumptions and caveats on large-scale, long-term compilations of plankton data

The biomass data used in this study are the most comprehensive available for Southern Ocean plankton groups. Nonetheless they have some limitations. We applied fixed conversion factors to the Chl *a*, mesoplankton, krill, and salp data to estimate the epipelagic carbon biomass, but in reality, these factors can vary regionally. For example, shallow mixed layer depths in ice-meltwater lenses and sheltered nearshore environments would reduce the conversion factor from surface Chl *a* concentration to a depth-integrated value (Korb et al. 2012). Likewise inshore phytoplankton blooms may

Fig. 7. Mean and SE of carbon biomass of mesozooplankton, krill and salps in MPA planning domains 1, 2, 4, and 7. Number of records in each era is shown on top of each error bar.

they can on occasion be caught in the Bongo and ring nets used for mesozooplankton collections. Given that the many small euphausiids (e.g., *Thysanoessa* spp.) are adept at escaping Bongo-type nets particularly in daytime, we suggest that our "mesozooplankton" value actually pertains to the metazoan mesozooplankton large enough to be retained on a 200 μm mesh, plus a variable portion of the smaller macroplankton (> 20 mm) assemblage, such as small euphausiids, chaetognaths, amphipods, pteropods, and gelatinous zooplankton (Ward et al. 2006). It is thus important to stress that this fraction contains a portion of larger, more carnivorous macroplankton as well as the true mesozooplankton, dominated by more herbivorous taxa such as copepods. In any case, with the higher rate of turnover as well as greater biomass of this "mesozooplankton" size fraction, their production would greatly exceed that of krill (Voronina 1998; Shreeve et al. 2005).

An important issue affecting compiled datasets and comparisons of data collected using different methods is that differences in sampling methodology, timing, location or sample size may influence the resulting estimates. In particular, the available data in some planning domains (e.g., domains 3, 6) are relatively sparse or restricted to productive islands (Fig. 1), potentially leading to overestimation at the scale of the whole planning domain. We have attempted to minimize the influence of these differences on analyses of the krill data and have used the resulting standardized values (Atkinson et al. 2008, 2017) here. For all datasets we have increased the comparability of data by using only those collected in the epipelagic layer and in the summer period, using common units and ensuring that all averages are based on at least 40 data points in each MPA planning domain (Fig. 1). Our averages are the current best available estimates of long-term average biomass.

Implications of high grazer biomass for the biological carbon pump and food chain efficiency

Polar oceans are characterized by very high biomass densities of mesoplankton and macroplankton (Biard et al. 2016; Moriarty and O'Brien 2013). In the Southern Ocean, Antarctic krill and salps have received more attention than the smaller mesozooplankton for their roles in nutrient cycling and in the biological carbon pump (BCP), due to their swarming ability, extraordinarily high biomass, rapid reproduction in favorable conditions, extensive vertical migrations, and fast-sinking fecal pellets, molts, and carcasses (Belcher et al. 2019; Cavan et al. 2019; Manno et al. 2020; Pakhomov et al. 2006; Schmidt et al. 2016). The relative roles of the major taxa are under debate (Bockmann et al. 2021) and Figs. 4–6 show that these will vary greatly with latitude and longitude due to the contrasts in their relative biomass.

Mesozooplankton, however, are also important in nutrient regeneration (Laglera et al. 2017) and many of the biomass-dominant mesozooplankton taxa, alongside Antarctic krill, salps, and chaetognaths, perform extensive seasonal vertical

reduce the carbon: Chl *a* ratio to values nearer 20 (Roy et al. 2017). Together, these factors will reduce the conversion from surface Chl *a* concentration into a depth-integrated phytoplankton carbon m^{-2}, potentially resulting in an overestimate of the phytoplankton standing stock in this study.

In addition, there is the potential for the mesozooplankton biomass values to have been over-estimated. Swarming of larger macroplankton (krill, salps, and *Themisto*) may be included in some of the mesozooplankton biomasses, since

migrations (Mackintosh 1937; Andrews 1966; Foxton 1966; Siegel 2005). In the northern hemisphere Jónasdóttir et al. (2015) quantified the "lipid pump" whereby seasonal vertical migration of *Calanus finmarchicus* transports lipids to the deep ocean where they are released through respiration, thus constituting an efficient sequestration pathway. They estimated that this flux of carbon, without concomitant loss of limiting nutrients, almost doubled existing BCP fluxes for the north Atlantic. In the Southern Ocean there has not yet been a comprehensive estimate of carbon flux via respiration and mortality of the entire assemblage that migrate seasonally, although estimates have been made for individual species (Bradford-Grieve et al. 2001; Shreeve et al. 2005). We suggest that the circumpolar mesozooplankton data that we provide (Supporting Information Data S1), alongside those for krill and salps, now allow such calculations. For a rough indicative estimate of the potential magnitude of this migratory flux, we use estimates from Atkinson et al. (1997) and Shreeve et al. (2005), that 75% of the overwintering *Calanoides acutus* population die at depth. As a simple calculation, applying this loss rate to the entire summer biomass of mesozooplankton (67 Mt) would yield a carbon export to depth of 50 Mt yr^{-1}. This estimate does not include the respiration of lipid at depth by mesozooplankton, krill, or salps. Thus, the combined value is probably large; for comparison the fecal pellet carbon export flux from krill in the marginal ice zone was estimated at 39 Mt yr^{-1} (Belcher et al. 2019). The combined effect of seasonal migrations, respiration, and mortality of such a large standing stock of mesozooplankton, krill, and salps across the Southern Ocean has major implications for the functioning of the BCP that need to be better quantified.

In addition to their role in carbon export, a large and migratory mesozooplankton and macrozooplankton biomass in the Southern Ocean has a profound influence on food web structure and function (Le Quéré et al. 2016). The combined biomass of grazers exceeded that of phytoplankton in all planning domains except domain 3, and mesozooplankton biomass alone exceeded that of phytoplankton in 7 of the 9 domains (Fig. 6). Such "top heavy" biomass pyramids (i.e., those in which the consumer biomass exceeds resource biomass; McCauley et al. 2018, sometimes called "inverted biomass pyramids") have been found in a variety of marine communities, from plankton to reef predators (McCauley et al. 2018). Mechanisms that could explain top heaviness include rapid turnover rates of phytoplankton, high transfer efficiency between primary producers and herbivores, high predator : prey mass ratios (PPMR), moderate levels of omnivory, intermediate levels of food web connectance, extra-community foraging and the use of multiple habitats and resources by mobile consumers like sharks (Shurin et al. 2006; Trebilco et al. 2013; McCauley et al. 2018). Assuming a community mean trophic efficiency of approximately 10%, inverted pyramids should occur when PPMR is higher than 4000 (Trebilco et al. 2013). This is often the case in the

Southern Ocean where the individual carbon biomass of small copepods (length about 1 mm) is approximately 4000 times the median individual carbon biomass of phytoplankton. The ratio rises to around 40,000,000 when krill is the grazer (Supporting Information Data S4). Substantial omnivory in the Southern Ocean zooplankton community could also promote top heaviness (McCauley et al. 2018), as could plankton systems with much shorter generation times and higher turnover rates of phytoplankton producers than zooplankton grazers (Shurin et al. 2006). These mechanisms, especially the high PPMRs, may explain the prevalence of inverted biomass pyramids in the Southern Ocean (Fig. 3).

Perspectives for spatial planning and management

AES for air-breathing predators were defined at a circumpolar scale based on tracking data (Hindell et al. 2020). These are clearly strong candidate areas for protection, but they pertain to a small fraction of the total biomass encompassing only the highest trophic levels (Hindell et al. 2020). Although the AESs are generally located in areas of high prey biomass around sub-Antarctic islands and on the Antarctic continental shelf (Fig. 2), they provide limited information on the low trophic level species which support the rest of the food web. By contrast, bioregions or biogeochemical regions are usually identified based on abiotic factors owning to the insufficiency of biotic data at large scale (Hill et al. 2017). Our circumpolar scale mapping of the basal trophic levels therefore fills the gap between the abiotic-based and predator-based views, supporting progress towards a more complete eco-regionalization for future ecosystem-based protection planning and management.

The balance of the four trophic groups showed great geographic contrasts among the 9 MPA planning domains (Figs. 5, 6). In contrast to the Atlantic sector (e.g., domain 2 near South Georgia and Scotia Sea) with overwhelming dominance of krill (Fig. 6), the low latitude regions of the Indian sector (e.g., planning domains 5 and 6 including Kerguelen Islands and Heard Island) are characterized by high-nutrient low-chlorophyll with pockets of natural iron-fertilized productivity, non-krill or low-krill but high-mesozooplankton systems (D'Ovidio et al. 2015). These spatial differences in composition and biomass of the plankton trophic groups suggest functionally different foodwebs across various MPA planning domains. Brooks et al. (2020) suggested that this full spectrum of food web functionality should be represented in a future circumpolar-scale network of protection.

Through carbon capture, fixation, and storage by marine organisms, blue carbon (carbon stored by the oceans and coastal ecosystems) is increasingly recognized as a critical ecosystem service of the Southern Ocean that warrants preservation (Cavanagh et al. 2021). Climate change was suggested to have complex effects on the high latitude blue carbon ecosystem services (Barnes et al. 2018). On one hand, coastal habitats efficient at storing blue carbon are decreasing in area over most of the world except polar regions where they are

increasing, driven by sea ice declines, glacier retreat, and ice collapse (Cavanagh et al. 2021). Areas with ice losses, such as in west Antarctica, can become new hotspots of blue carbon owing to the longer algal blooms and increasing benthic carbon storage with negative feedback to climate change (Barnes et al. 2018; Pineda-Metz et al. 2020). On the other hand, warming or declines in sea ice may change the relative fortunes of all biomass-dominant grazers such as mesozooplankton, krill, and salps (Ward et al. 2018) which play strong roles in the blue carbon pathway (Cavan et al. 2019; Pauli et al. 2021). Distribution centers of Antarctic krill have contracted southward towards the Antarctic continent where new spawning hotspots of krill developed during rapid warming (Atkinson et al. 2019, 2021), while salps seem to be expanding in the same direction (Pakhomov et al. 2002; Atkinson et al. 2004). This suggests that the carbon sequestration potential of these key shelf habitats should be a major consideration in conservation efforts.

Climate change and alterations in the physical environment (e.g., increasing temperature, changes in the extent and seasonality of ice, high frequency of positive Southern Annular Mode) are driving changes in Southern Ocean ecosystems (Rogers et al. 2020). Although Earth Observation and Argo floats have helped to increase the scales at which physical and biogeochemical parameters, including primary production, can be observed (Claustre et al. 2020), modern sampling technology has paradoxically reduced the focal scales of zooplankton studies (Picheral et al. 2010; Whitmore and Ohman 2021). To examine plankton at scales relevant to climate change, net-based zooplankton sampling needs to be continued, in order to extend existing time series. This has not happened, since nets at pre-fixed stations are being used far less in modern times (Fig. 7). Increased synthesis of existing large-scale, net-based data on the zooplankton trophic groups could help the circumpolar scale perspective needed both for future ecosystem-based protection and for carbon budgets and models of the changing marine ecosystems around Antarctica.

Data availability statement

The data supporting the findings of this study are available within the supplementary materials.

References

Andrews, K. J. H. 1966. The distribution and life-history of *Calanoides acutus* (Giesbrecht). Discov. Rep. **34**: 117–162.

Arrigo, K. R., G. L. van Dijken, and S. Bushinsky. 2008. Primary production in the Southern Ocean, 1997–2006. J. Geophys. Res. Oceans **113**: C08004. doi:10.1029/2007JC004551

Atkinson, A. 1991. Life cycle of *Calanoides acutus*, *Calanus simillimus* and *Rhincalanus gigas* (Copepoda: Calanoida) within the Scotia Sea. Mar. Biol. **109**: 79–91. doi:10.1007/BF01320234

Atkinson, A., S. B. Schnack-Schiel, P. Ward, and V. Marin. 1997. Regional differences in the life cycle of *Calanoides acutus* (Copepoda: Calanoida) within the Atlantic sector of the Southern Ocean. Mar. Ecol. Prog. Ser. **150**: 99–111. doi:10.3354/meps150099

Atkinson, A., V. Siegel, E. A. Pakhomov, and P. Rothery. 2004. Long-term decline in krill stock and increase in salps within the Southern Ocean. Nature **432**: 100–103. doi:10.1038/nature02996

Atkinson, A., and others. 2008. Oceanic circumpolar habitats of Antarctic krill. Mar. Ecol. Prog. Ser. **362**: 1–23. doi:10.3354/meps07498

Atkinson, A., V. Siegel, E. A. Pakhomov, M. J. Jessopp, and V. Loeb. 2009. A re-appraisal of the total biomass and annual production of Antarctic krill. Deep Sea Res. Pt. I **56**: 727–740. doi:10.1016/j.dsr.2008.12.007

Atkinson, A., P. Ward, B. P. V. Hunt, E. A. Pakhomov, and G. W. Hosie. 2012. An overview of Southern Ocean zooplankton data: Abundance, biomass, feeding and functional relationships. CCAMLR Sci. **19**: 171–218. doi:10.1051/kmae/2012006

Atkinson, A., and others. 2017. KRILLBASE: A circumpolar database of Antarctic krill and salp numerical densities, 1926–2016. Earth Syst. Sci. Data **9**: 193–210. doi:10.5194/essd-2016-52

Atkinson, A., and others. 2019. Krill (*Euphausia superba*) distribution contracts southward during rapid regional warming. Nat. Clim. Change **9**: 142–147. doi:10.1038/s41558-018-0370-z

Atkinson, A., and others. 2021. Stepping stones towards Antarctica: Switch to southern spawning grounds explains an abrupt range shift in krill. Glob. Chang. Biol. **28**: 1359–1375. doi:10.1111/gcb.16009

Balvay, P. G. 1987. Equivalence entre quelques parametres estimatifs de I'abondance du zooplankton total. Schweiz. Z. Hydrol **49**: 75–83.

Barnes, D. K. A., A. Fleming, C. J. Sands, M. L. Quartino, and D. Deregibus. 2018. Icebergs, sea ice, blue carbon and Antarctic climate feedbacks. Philos. Trans. R. Soc. A Math. Phys. Eng. Sci. **376**: 20170176. doi:10.1098/rsta.2017.0176

Belcher, A., and others. 2019. Krill faecal pellets drive hidden pulses of particulate organic carbon in the marginal ice zone. Nat. Commun. **10**: 889. doi:10.1038/s41467-019-08847-1

Biard, T., and others. 2016. In situ imaging reveals the biomass of giant protists in the global ocean. Nature **532**: 504–507. doi:10.1038/nature17652

Bockmann, S., and others. 2021. Salp fecal pellets release more bioavailable iron to Southern Ocean phytoplankton than krill fecal pellets. Curr. Biol. **31**: 2737–2746. doi:10.1016/j.cub.2021.02.033

Bradford-Grieve, J. M., S. D. Nodder, J. B. Jillett, K. Currie, and K. R. Lassey. 2001. Potential contribution that the copepod *Neocalanus tonsus* makes to downward carbon flux in the

Southern Ocean. J. Plankton Res. **23**: 963–975. doi:10.1093/plankt/23.9.963

Brooks, C. M., S. L. Chown, L. L. Douglass, B. P. Raymond, J. D. Shaw, A. T. Sylvester, and C. L. Torrens. 2020. Progress towards a representative network of Southern Ocean protected areas. PLoS One **15**: e0231361. doi:10.1371/journal.pone.0231361

Cavan, E. L., and others. 2019. The importance of Antarctic krill in biogeochemical cycles. Nat. Commun. **10**: 4742. doi:10.1038/s41467-019-12668-7

Cavanagh, R. D., and others. 2021. Future risk for Southern Ocean ecosystem services under climate change. Front. Mar. Sci. **7**: 615214. doi:10.3389/fmars.2020.615214

Claustre, H., K. S. Johnson, and Y. Takeshita. 2020. Observing the global ocean with biogeochemical-Argo. Ann. Rev. Mar. Sci. **12**: 23–48. doi:10.1146/annurev-marine-010419-010956

D'Ovidio, F., and others. 2015. The biogeochemical structuring role of horizontal stirring: Lagrangian perspectives on iron delivery downstream of the Kerguelen Plateau. Biogeosciences **12**: 5567–5581. doi:10.5194/bg-12-5567-2015

Deppeler, S. L., and A. T. Davidson. 2017. Southern ocean phytoplankton in a changing climate. Front. Mar. Sci. **4**: 40. doi:10.3389/fmars.2017.00040

Dubischar, C. D., E. A. Pakhomov, L. von Harbou, B. P. V. Hunt, and U. V. Bathmann. 2012. Salps in the Lazarev Sea, Southern Ocean: II. Biological composition and potential prey value. Mar. Biol. **159**: 15–24. doi:10.1007/s00227-011-1785-5

Foxton, P. 1956. The distribution of the standing crop of zooplankton in the Southern Ocean. Discov. Rep. **28**: 191–236.

Foxton, P. 1966. The distribution and life history of *Salpa thompsoni* Foxton, with observations on a related species, *Salpa gerlachei* Foxton. Discov. Rep. **34**: 1–116.

Gallienne, C. P., and D. B. Robins. 2001. Is *Oithona* the most important copepod in the world's oceans? J. Plankton Res. **23**: 1421–1432. doi:10.1093/plankt/23.12.1421

Hill, N. A., S. D. Foster, G. Duhamel, D. Welsford, P. Koubbi, and C. R. Johnson. 2017. Model-based mapping of assemblages for ecology and conservation management: A case study of demersal fish on the Kerguelen Plateau. Divers. Distrib. **23**: 1216–1230. doi:10.1111/ddi.12613

Hill, S. L., M. H. Pinkerton, T. Ballerini, E. L. Cavan, L. J. Gurney, I. Martins, and J. C. Xavier. 2021. Robust model-based indicators of regional differences in food-web structure in the Southern Ocean. J. Marine Syst. **220**: 103556. doi:10.1016/j.jmarsys.2021.103556

Hindell, M. A., and others. 2020. Tracking of marine predators to protect Southern Ocean ecosystems. Nature **580**: 87–92. doi:10.1038/s41586-020-2126-y

Johnson, N. M., and others. 2022. Status, change and futures of zooplankton in the Southern Ocean. Front. Ecol. Evol. **9**: 624692. doi:10.3389/fevo.2021.624692

Jónasdóttir, S. H., W. V. Andre, R. Katherine, and R. H. Michael. 2015. Seasonal copepod lipid pump promotes carbon sequestration in the deep North Atlantic. Proc. Natl. Acad. Sci. USA **112**: 12122–12126. doi:10.1073/pnas.1512110112

Karakus, O., C. Volker, M. Iversen, W. Hagen, D. Wolf-Gladrow, B. Fach, and J. Hauck. 2021. Modelling the impact of microzooplankton on carbon export production in the Southern Ocean. J. Geophys. Res. Oceans **126**: e2021JC017315. doi:10.1029/2021JC017315

Kawamura, A. 1986. Has marine Antarctic ecosystem changed?—A tentative comparison of present and past microzooplankton abundances. Mem. Natl. Inst. Polar Res. **40**: 197–211.

Korb, R. E., M. J. Whitehouse, P. Ward, M. Gordon, H. J. Venables, and A. J. Poulton. 2012. Regional and seasonal differences in microplankton biomass, productivity, and structure across the Scotia Sea: Implications for the export of biogenic carbon. Deep-Sea Res. Pt. II **59–60**: 67–77. doi:10.1016/j.dsr2.2011.06.006

Laglera, L. M., and others. 2017. Iron partitioning during LOHAFEX: Copepod grazing as a major driver for iron recycling in the Southern Ocean. Mar. Chem. **196**: 148–161. doi:10.1016/j.marchem.2017.08.011

Le Quéré, C., and others. 2016. Role of zooplankton dynamics for Southern Ocean phytoplankton biomass and global biogeochemical cycles. Biogeosciences **13**: 4111–4413. doi:10.5194/bg-13-4111-2016

Mackintosh, N. A. 1937. The seasonal circulation of the Antarctic macroplankton. Discov. Rep. **16**: 365–412.

Manno, C., S. Fielding, G. Stowasser, E. J. Murphy, S. E. Thorpe, and G. A. Tarling. 2020. Continuous moulting by Antarctic krill drives major pulses of carbon export in the north Scotia Sea, Southern Ocean. Nat. Commun. **11**: 6051. doi:10.1038/s41467-020-19956-7

Marr, J. 1962. The natural history and geography of the Antarctic krill (*Euphausia superba* Dana). Discov. Rep. **10**: 33–464.

McCauley, D. J., G. Gellner, N. D. Martinez, R. J. Williams, S. A. Sandin, F. Micheli, P. J. Mumby, and K. S. McCann. 2018. On the prevalence and dynamics of inverted trophic pyramids and otherwise top-heavy communities. Ecol. Lett. **21**: 439–454. doi:10.1111/ele.12900

McCormack, S. A., J. Melbourne-Thomas, R. Trebilco, J. L. Blanchard, B. Raymond, and A. Constable. 2021. Decades of dietary data demonstrate regional food web structures in the Southern Ocean. Ecol. Evol. **11**: 227–241. doi:10.1002/ece3.7017

Mélin, F., V. Vantrepotte, A. Chuprin, M. Grant, T. Jackson, and S. Sathyendranath. 2017. Assessing the fitness-for-purpose of satellite multi-mission ocean color climate data records: A protocol applied to OC-CCI. Remote Sens. Environ. **203**: 139–151. doi:10.1016/j.rse.2017.03.039

Moriarty, R., and T. D. O'Brien. 2013. Distribution of mesozooplankton biomass in the global ocean. Earth Syst. Sci. Data **5**: 45–55. doi:10.5194/essd-5-45-2013

Morley, S. A., and others. 2020. Global drivers on Southern Ocean ecosystems: Changing physical environments and anthropogenic pressures in an earth system. Front. Mar. Sci. **7**: 547188. doi:10.3389/fmars.2020.547188

Murphy, E. J., and others. 2021. Global connectivity of Southern Ocean ecosystems. Front. Ecol. Evol. **9**: 624451. doi:10.3389/fevo.2021.624451

Orsi, A. H., T. Whitworth, and W. D. Nowlin. 1995. On the meridional extent and fronts of the Antarctic circumpolar current. Deep Sea Res. Part I **42**: 641–673. doi:10.1016/0967-0637(95)00021-W

Pakhomov, E. A., P. W. Froneman, and R. Perissinotto. 2002. Salp/krill interactions in the Southern Ocean: Spatial segregation and implications for the carbon flux. Deep Sea Res. Part II **49**: 1881–1907. doi:10.1016/S0967-0645(02)00017-6

Pakhomov, E. A., C. D. Dubischar, V. Strass, M. Brichta, and U. V. Bathmann. 2006. The tunicate *Salpa thompsoni* ecology in the Southern Ocean. I. Distribution, biomass, demography and feeding ecophysiology. Mar. Biol. **149**: 609–623. doi:10.1007/s00227-005-0225-9

Parkinson, C. L., and D. J. Cavalieri. 2012. Antarctic Sea ice variability and trends, 1979–2010. Cryosphere **6**: 871–880. doi:10.5194/tc-6-871-2012

Pauli, N., and others. 2021. Krill and salp faecal pellets contribute equally to the carbon flux at the Antarctic Peninsula. Nat. Commun. **12**: 7168. doi:10.1038/s41467-021-27436-9

Picheral, M., L. Guidi, L. Stemmann, D. M. Karl, G. Iddaoud, and G. Gorsky. 2010. The Underwater Vision Profiler 5: An advanced instrument for high spatial resolution studies of particle size spectra and zooplankton. Limnol. Oceanogr. Methods **8**: 462–473. doi:10.4319/lom.2010.8.462

Pineda-Metz, S. E. A., D. Gerdes, and C. Richter. 2020. Benthic fauna declined on a whitening Antarctic continental shelf. Nat. Commun. **11**: 2226. doi:10.1038/s41467-020-16093-z

Pinkerton, M. H., M. Decima, J. Kitchener, K. Takahashi, K. Robinson, R. Stewart, and G. Hosie. 2020. Zooplankton in the Southern Ocean form the continuous plankton recorder: Distributions and long-term change. Deep Sea Res. Part I **162**: 103303. doi:10.1016/j.dsr.2020.103303

Pinkerton, M. H., P. W. Boyd, S. Deppler, A. Hayward, J. Hofer, and S. Moreau. 2021. Evidence for the impact of climate change on primary producers in the Southern Ocean. Front. Ecol. Evol. **9**: 592027. doi:10.3389/fevo.2021.592027

Ratcliffe, N., and others. 2021. Changes in prey fields increase the potential for spatial overlap between gentoo penguins and a krill fishery within a marine protected area. Divers. Distrib. **27**: 552–563. doi:10.1111/ddi.13216

Raymond, R. 2011. A circumpolar pelagic regionalisation of the Southern Ocean. CCAMLR Workshop on Marine Protected Areas (Brest, France, 29 August to 2 September 2011). Document WS-MPA-11/6. Available from http://data.aad.gov.au/regionalisation

Rogers, A. D., and others. 2020. Antarctic futures: An assessment of climate-driven changes in ecosystem structure, function, and service provisioning in the Southern Ocean. Ann. Rev. Mar. Sci. **12**: 87–120. doi:10.1146/annurev-marine-010419-011028

Roy, S., S. Sathyendranath, and T. Platt. 2017. Size-partitioned phytoplankton carbon and carbon-to-chlorophyll ratio from coean colour by an absorption-based bio-optical algorithm. Remote Sens. Environ. **194**: 177–189. doi:10.1016/j.rse.2017.02.015

Sathyendranath, S., and others. 2009. Carbon-to-chlorophyll ratio and growth rate of phytoplankton in the sea. Mar. Ecol. Prog. Ser. **383**: 73–84. doi:10.3354/meps07998

Sathyendranath, S., and others. 2019. An ocean-colour time series for use in climate studies: The experience of the Ocean-Colour Climate Change Initiative (OC-CCI). Sensors **19**: 4285. doi:10.3390/s19194285

Schlitzer, R. 2021. Ocean data view. Available from https://odv.awi.de

Schmidt, K., C. Schlosser, A. Atkinson, S. Fielding, H. J. Venables, C. M. Waluda, and E. P. Achterberg. 2016. Zooplankton gut passage mobilizes lithogenic iron for ocean productivity. Curr. Biol. **26**: 2667–2673. doi:10.1016/j.cub.2016.07.058

Shreeve, R. S., G. A. Tarling, A. Atkinson, P. Ward, C. Goss, and J. Watkins. 2005. Relative production of *Calanoides acutus* (Copepoda: Calanoida) and *Euphausia superba* (Antarctic krill) at South Georgia, and its implications at wider scales. Mar. Ecol. Prog. Ser. **298**: 229–239. doi:10.3354/meps298229

Shurin, J. B., D. S. Gruner, and H. Hillebrand. 2006. All wet or dried up? Real differences between aquatic and terrestrial food webs. Proc. Roy. Soc. B Biol. Sci. **273**: 1–9. doi:10.1098/rspb.2005.3377

Siegel, V. 2005. Distribution and population dynamics of *Euphausia superba*: Summary of recent findings. Polar Biol. **29**: 1–22. doi:10.1007/s00300-005-0058-5

Stammerjohn, S., R. Massom, D. Rind, and D. Martinson. 2012. Regions of rapid sea ice change: An inter-hemispheric seasonal comparison. Geophy. Res. Lett. **39**: L06501. doi:10.1029/2012GL050874

Teschke, K., H. Pehlke, V. Siegel, H. Bornemann, R. Knust, and T. Brey. 2020. An integrated compilation of data sources for the development of a marine protected area in the Weddell Sea. Earth Syst. Sci. Data **12**: 1003–1023. doi:10.5194/essd-12-1003-2020

Trebilco, R., J. K. Baum, A. K. Salomon, and N. K. Dulvy. 2013. Ecosystem ecology: Size-based constraints on the pyramids of life. Trends Ecol. Evol. **28**: 423–431. doi:10.1016/j.tree.2013.03.008

Voronina, N. M. 1998. Comparative abundance and distribution of major filter-feeders in the Antarctic pelagic zone. J. Mar. Syst. **17**: 375–390. doi:10.1016/S0924-7963(98)00050-5

Ward, P., R. Shreeve, A. Atkinson, B. Korb, M. Whitehouse, S. Thorpe, D. Pond, and N. Cunningham. 2006. Plankton community structure and variability in the Scotia Sea: Austral summer 2003. Mar. Ecol. Prog. Ser. **309**: 75–91. doi:10.3354/meps309075

Ward, P., G. A. Tarling, and S. E. Thorpe. 2018. Temporal changes in abundances of large calanoid copepods in the Scotia Sea: Comparing the 1930s with contemporary times. Polar Biol. **41**: 2297–2310. doi:10.1007/s00300-018-2369-3

Whitmore, B. M., and M. D. Ohman. 2021. Zooglider-measured association of zooplankton with the fine-scale vertical prey field. Limnol. Oceanogr. **66**: 3811–3827. doi:10.1002/lno.11920

Wiebe, P. H. 1988. Functional regression equations for zooplankton displacement volume, wet weight, dry weight, and carbon. A correction. Fish. Bull. **86**: 833–835.

Yang, G., A. Atkinson, S. L. Hill, L. Guglielmo, A. Granata, and C. Li. 2020. Changing circumpolar distributions and iso-scapes of Antarctic krill: Indo-Pacific habitat refuges counter long-term degradation of the Atlantic sector. Limnol. Oceanogr. **66**: 272–287. doi:10.1002/lno.11603

Conflict of Interest

None declared.